

Polarization and dilepton angular distribution in pion-nucleon collisions

Miklós Zétényi · Enrico Speranza · Bengt Friman

Received: date / Accepted: date

Abstract We study hadronic polarization and the related anisotropy of the dilepton angular distribution for the reaction $\pi N \rightarrow Ne^+e^-$. We employ consistent effective interactions for baryon resonances up to spin-5/2 to compute their contribution to the anisotropy coefficient. We show that the spin and parity of the intermediate baryon resonance is reflected in the angular dependence of the anisotropy coefficient. We present results for the anisotropy coefficient including the $N(1520)$ and $N(1440)$ resonances, which are essential at the collision energy of the recent data obtained by the HADES collaboration on this reaction. We conclude that the anisotropy coefficient provides useful constraints for unraveling the resonance contributions to this process.

Keywords Polarization · angular distribution · dilepton production

PACS 13.75.Gx · 13.88.+e · 14.20.Gk

1 Introduction

Dilepton production in hadronic reactions provides information on the electromagnetic properties of hadrons. Dileptons are produced in a variety of different elementary processes. Independently of the specific reaction, they originate from the decay of virtual photons. Multiply differential cross sections for dilepton production can provide information that may help to disentangle the production channels.

The HADES collaboration has recently studied dilepton production in pion-induced reactions [1]. One of the most important contributions to this reaction

Miklós Zétényi
Wigner Research Center for Physics, H-1121 Budapest, Hungary
E-mail: zetenyi.miklos@wigner.mta.hu

Enrico Speranza
Institut für Theoretische Physik, Goethe-Universität, D-60438 Frankfurt am Main, Germany

Bengt Friman
GSI Helmholtzzentrum für Schwerionenforschung GmbH, D-64291 Darmstadt, Germany

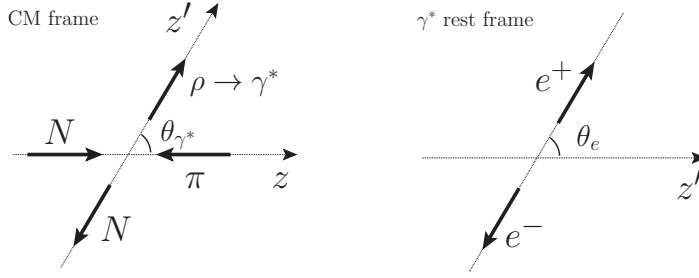


Fig. 1 Definition of the angles in the CM frame and the virtual photon rest frame.

originates from processes with intermediate s -channel baryon resonances, $\pi N \rightarrow R \rightarrow Ne^+e^-$. In this presentation we explore the baryonic contributions to the reaction $\pi N \rightarrow Ne^+e^-$ in terms of an effective Lagrangian model at the center-of-momentum (CM) energy of the HADES experiment. In particular, we study the angular distribution of the produced dileptons, which reflects the polarization state of the decaying virtual photon, and, ultimately, carries information about the process in which the virtual photon was created. In the present case, the polarization data provides constraints on the quantum numbers of the intermediate baryon resonances. This contribution is based on our previous publication [2], where the interested reader can find further details.

The general expression for the triple differential cross section of the process $\pi N \rightarrow Ne^+e^-$ is

$$\frac{d\sigma}{dM d\cos\theta_{\gamma^*} d\cos\theta_e} \propto \Sigma_{\perp}(1 + \cos^2\theta_e) + \Sigma_{\parallel}(1 - \cos^2\theta_e) \\ \propto A(1 + \lambda_{\theta}(\theta_{\gamma^*}, M) \cos^2\theta_e), \quad (1)$$

where M is the mass of the virtual photon (the dilepton invariant mass), θ_{γ^*} is the virtual photon polar angle in the CM frame, and θ_e is the polar angle of one of the two leptons in the rest frame of the photon as measured relative to the momentum of the virtual photon in the CM frame. This choice is called the helicity frame (see Fig. 1). In the second line we defined the anisotropy coefficient

$$\lambda_{\theta}(\theta_{\gamma^*}, M) = \frac{\Sigma_{\perp} - \Sigma_{\parallel}}{\Sigma_{\perp} + \Sigma_{\parallel}}, \quad (2)$$

which contains information on the polarization of the virtual photon and hence on the reaction mechanism.

The emergence of a dilepton anisotropy in the process $\pi N \rightarrow R \rightarrow Ne^+e^-$ can be understood as follows. The initial state, which in the CM frame contains a pion with momentum \mathbf{p} and a nucleon with momentum $-\mathbf{p}$, can be expanded in terms of eigenstates of orbital angular momentum

$$|\pi(\mathbf{p}); N(-\mathbf{p})\rangle \propto \sum_{lm} Y_{lm}^*(\theta, \phi) |lm\rangle, \quad (3)$$

where θ and ϕ specify the direction of \mathbf{p} with respect to the quantization axis. We choose the quantization axis z parallel to the momentum of the incident

pion, implying that $\theta = 0$. In this case the z -component of the orbital angular momentum vanishes in the initial state. Hence, the projection of the total spin of the intermediate baryon resonance on the beam axis is the same as the z -component of the nucleon spin. This means that only the $J_z = +1/2$ and $-1/2$ states of the resonance are populated.

As a result, in case of an unpolarized nucleon target, spin-1/2 intermediate resonances are unpolarized, and consequently there is no preferred direction in the CM frame. Accordingly, in this case all observables are independent of the scattering angle, i.e., the angle θ_{γ^*} of the virtual photon in the CM frame. On the other hand, intermediate resonances of spin $\geq 3/2$ have a nontrivial polarization, implying an angular anisotropy in the CM frame. Consequently, in this case, observables show a nontrivial dependence on the scattering angle θ_{γ^*} , which reflects the quantum numbers of the resonance.

2 Cross section and anisotropy coefficient

The matrix element of the process $\pi N \rightarrow Ne^+e^-$ can be decomposed as a product of a leptonic part, describing the decay of the virtual photon, and a hadronic part, containing the rest of the process including the production of the virtual photon. Consequently, the square of the matrix element can be written in the form

$$\sum_{\text{pol}} |\mathcal{M}|^2 = \frac{e^2}{k^4} W_{\mu\nu} l^{\mu\nu}, \quad (4)$$

where the lepton tensor, $l^{\mu\nu}$, is determined by the leptonic matrix element. Its explicit form is easily obtained from quantum electrodynamics, as

$$l^{\mu\nu} = 4 \left[k_1^\mu k_2^\nu + k_1^\nu k_2^\mu - (k_1 \cdot k_2 + m_e^2) g^{\mu\nu} \right], \quad (5)$$

where k_1 and k_2 are the momenta of the electron and positron, respectively, and m_e is the electron mass. The quantity

$$W_{\mu\nu} = \sum_{\text{pol}} \mathcal{M}_\mu^{\text{had}} \mathcal{M}_\nu^{\text{had}*} \quad (6)$$

is the hadronic tensor, expressed in terms of the hadronic matrix element, $\mathcal{M}_\mu^{\text{had}}$.

It is convenient to introduce the polarization density matrix formalism [4]. The hadronic (or production) density matrix is defined as

$$\rho_{\lambda\lambda'}^{\text{had}} = \frac{e^2}{k^4} \epsilon^\mu(k, \lambda) W_{\mu\nu} \epsilon^\nu(k, \lambda')^*, \quad (7)$$

and it represents the polarization state of the virtual photon produced in the hadronic part of the reaction. The leptonic (or decay) density matrix is defined as

$$\rho_{\lambda'\lambda}^{\text{lep}} = \epsilon^\mu(k, \lambda') l_{\mu\nu} \epsilon^\nu(k, \lambda)^*, \quad (8)$$

and it projects the above state of the virtual photon on the final state containing the lepton pair. In the above, $\epsilon^\mu(k, \lambda)$ denotes the polarization vector of the virtual photon of momentum k and helicity λ . The latter can take on values ± 1 and

0, since virtual photons can also be longitudinally polarized. In terms of the polarization density matrices, the square of the matrix element - which contains all the information about angular distributions - can be written as

$$\sum_{\text{pol}} |\mathcal{M}|^2 = \sum_{\lambda, \lambda'} \rho_{\lambda, \lambda'}^{\text{had}} \rho_{\lambda', \lambda}^{\text{lep}}. \quad (9)$$

Using the explicit form of the lepton tensor, Eq. 5, and neglecting the electron mass, the leptonic density matrix is obtained as

$$\rho_{\lambda', \lambda}^{\text{lep}} = 4|\mathbf{k}_1|^2 \begin{pmatrix} 1 + \cos^2 \theta_e & -\sqrt{2} \cos \theta_e \sin \theta_e e^{-i\phi_e} & \sin^2 \theta_e e^{-2i\phi_e} \\ -\sqrt{2} \cos \theta_e \sin \theta_e e^{i\phi_e} & 2(1 - \cos^2 \theta_e) & \sqrt{2} \cos \theta_e \sin \theta_e e^{-i\phi_e} \\ \sin^2 \theta_e e^{2i\phi_e} & \sqrt{2} \cos \theta_e \sin \theta_e e^{i\phi_e} & 1 + \cos^2 \theta_e \end{pmatrix}, \quad (10)$$

where \mathbf{k}_1 is the three-momentum of one of the two leptons in the virtual photon rest frame. The angular dependence of the squared matrix element is obtained by combining Eqs. (9) and (10),

$$\begin{aligned} \sum_{\text{pol}} |\mathcal{M}|^2 &\propto (1 + \cos^2 \theta_e)(\rho_{-1, -1}^{\text{had}} + \rho_{1, 1}^{\text{had}}) + 2(1 - \cos^2 \theta_e)\rho_{0, 0}^{\text{had}} \\ &+ \text{terms vanishing upon integration over } \phi_e. \end{aligned} \quad (11)$$

Here we suppressed the explicit dependence of $\rho_{\lambda, \lambda'}^{\text{had}}$ on M and θ_{γ^*} . By comparing Eqs. (1) and (11), we can identify the anisotropy coefficient

$$\lambda_\theta = \frac{\rho_{-1, -1}^{\text{had}} + \rho_{1, 1}^{\text{had}} - 2\rho_{0, 0}^{\text{had}}}{\rho_{-1, -1}^{\text{had}} + \rho_{1, 1}^{\text{had}} + 2\rho_{0, 0}^{\text{had}}}. \quad (12)$$

3 The effective Lagrangian model

In this section we specify the terms of the effective Lagrangian describing the interactions of all hadrons playing a role in the process. From this Lagrangian, transition matrix elements and also the hadronic density matrix can be calculated via standard Feynman diagram techniques.

We assume that baryons couple to the electromagnetic field via an intermediate ρ^0 meson according to the vector meson dominance model. For the ρ^0 -photon coupling we use the gauge invariant vector meson dominance model Lagrangian [5]

$$\mathcal{L}_{\rho\gamma} = -\frac{e}{2g_\rho} F^{\mu\nu} \rho_{\mu\nu}^0, \quad (13)$$

where $F^{\mu\nu} = \partial_\mu A_\nu - \partial_\nu A_\mu$ is the electromagnetic field strength tensor and $\rho_{\mu\nu}^0 = \partial_\mu \rho_\nu^0 - \partial_\nu \rho_\mu^0$.

We include baryon resonances up to spin-5/2. The interaction of spin-1/2 baryons with pions and ρ mesons is described by the Lagrangian densities of Ref. [3],

$$\mathcal{L}_{R_{1/2} N \pi} = -\frac{g_{RN\pi}}{m_\pi} \bar{\psi}_R \Gamma \gamma^\mu \boldsymbol{\tau} \psi_N \cdot \partial_\mu \boldsymbol{\pi} + \text{h.c.}, \quad (14)$$

$$\mathcal{L}_{R_{1/2} N \rho} = \frac{g_{RN\rho}}{2m_\rho} \bar{\psi}_R \boldsymbol{\tau} \sigma^{\mu\nu} \tilde{F} \psi_N \cdot \boldsymbol{\rho}_{\mu\nu} + \text{h.c.} \quad (15)$$

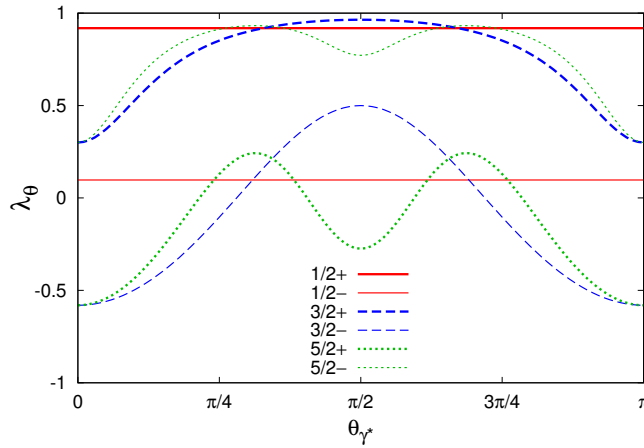


Fig. 2 The anisotropy coefficient λ_θ as a function of the virtual photon polar angle θ_{γ^*} for hypothetical resonance states with different spins and parities in the s -channel at a dilepton mass $M = 0.5$ GeV. The resonance masses coincide with $\sqrt{s} = 1.49$ GeV, the resonance widths are $\Gamma_R = 0.15$ GeV.

Here, and also in the Lagrangians involving higher spin resonances given below, $\Gamma = \gamma_5$ for $J^P = 1/2^+$, $3/2^-$ and $5/2^+$ resonances and $\Gamma = 1$ otherwise, and $\tilde{\Gamma} = \gamma_5 \Gamma$.

Higher spin fermions are represented by Rarita-Schwinger spinor fields in effective Lagrangian models. We include spin-3/2 and spin-5/2 resonances in our model and describe their interactions using the consistent interaction scheme developed by Vrancx et al. [6]. For details we refer to Ref. [2].

4 Results

We employ the model described above to compute the anisotropy coefficient λ_θ of Eq. (12) for the reaction $\pi N \rightarrow Ne^+e^-$. In the following we discuss the dependence of the anisotropy coefficient on the polar angle of the virtual photon θ_{γ^*} . In all the calculations, the CM energy is set to $\sqrt{s} = 1.49$ GeV, corresponding to the HADES data.

We explore the relevance of the different spins and parities by computing the anisotropy coefficient with a hypothetical resonance for each spin-parity combination, with mass $m_R = 1.49$ GeV and width $\Gamma_R = 0.15$ GeV. The mass was chosen to coincide with the CM energy \sqrt{s} used in our calculations, thus assuming that in the s -channel the resonance is on the mass shell. The results of this calculation for dileptons of invariant mass $M = 0.5$ GeV are shown in Fig. 2. Here one can see that the spin and parity of the intermediate resonance is reflected in a characteristic angular dependence of the anisotropy coefficient. In particular, in the spin-1/2 channels the λ_θ coefficient is independent of θ_{γ^*} , in accordance with the arguments given in the introduction.

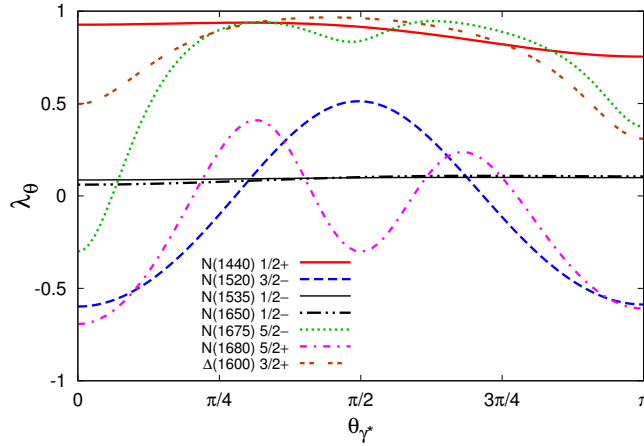


Fig. 3 Contributions of resonances to the anisotropy coefficient λ_θ as a function of the virtual photon polar angle at a dilepton mass $M = 0.5$ GeV including s - and u -channel diagrams. The CM energy is $\sqrt{s} = 1.49$ GeV. For further details, see the text.

In Fig. 3 we show the λ_θ coefficient obtained from the s - and u -channel diagrams of the physical resonance states that are relevant at the energy of the HADES experiment. Here, the characteristic shapes presented in Fig. 2 are modified by the interference with the u -channel resonance contributions and the off-shellness of the s -channel contributions.

In order to identify the resonances that are important for the dilepton production process at the CM energy of the HADES experiment, we compute the differential cross section $d\sigma/dM$ by integrating out the angles in the triple differential cross section of Eq. 1. For this calculation, the coupling constants $g_{RN\pi}$ and $g_{RN\rho}$ were determined from the widths of the $R \rightarrow N\pi$ and $R \rightarrow N\rho \rightarrow N\pi\pi$ decays. The empirical values for these partial widths were obtained as a product of the total width and the appropriate branching ratio as given by the Particle Data Group [7].

We found that at $\sqrt{s} = 1.49$ GeV and a dilepton invariant mass of $M = 0.5$ GeV, the two dominant contributions are due to the $N(1520)$ and $N(1440)$ resonances.

The double-differential cross section, $d\sigma/dM d\cos\theta_{\gamma^*}$ obtained from s - and u -channel diagrams with the dominant $N(1520)$ and $N(1440)$ resonances is shown in Fig. 4 as a function of the polar angle of the virtual photon, θ_{γ^*} . Here two of the curves correspond to the contributions of the two resonances without interference. In the other two, the interference terms are included, assuming either a positive or negative relative sign between the two resonance amplitudes. From Fig. 4 it is clear that the relative phase has a strong influence on the shape of the θ_{γ^*} dependence of the differential cross section.

In Fig. 5 we show the dominant contributions to the anisotropy coefficient λ_θ as a function of θ_{γ^*} . As in Fig. 4, we show results for the two limiting assumptions for the relative phase of the two resonance amplitudes. In both cases, the shape of the curve approximately follows that of the $N(1520)$ contribution, which implies that it is only weakly affected by the uncertainties of the $N(1440)$ parameters and the relative phase of the two amplitudes. The anisotropy parameter λ_θ has a maximum

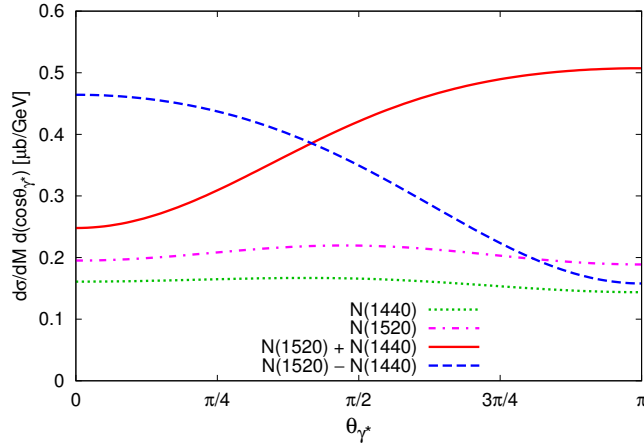


Fig. 4 The contribution of the two dominant resonances, $N(1440)$ and $N(1520)$, to the differential cross section of dilepton production at $\sqrt{s} = 1.49$ GeV CM energy and $M = 0.5$ GeV dilepton mass. For the explanation of the various curves, see the text.

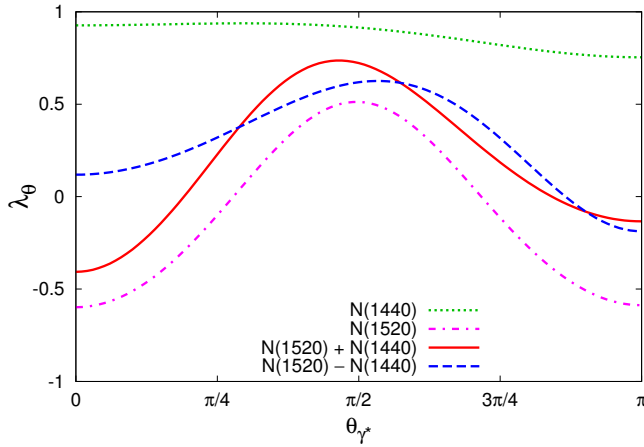


Fig. 5 The contribution of the two dominant resonances, $N(1440)$ and $N(1520)$, to the anisotropy coefficient, λ_θ at $\sqrt{s} = 1.49$ GeV CM energy and $M = 0.5$ GeV dilepton mass. The various curves correspond to the same assumptions as in Fig. 4

around $\theta_{\gamma^*} = \pi/2$, which means that virtual photons emitted perpendicular to the beam axis in the CM frame tend to be transversely polarized. On the other hand, virtual photons emitted along the beam direction are almost unpolarized or can even have some degree of longitudinal polarization.

5 Summary and outlook

In this contribution we studied the angular distribution of dileptons originating from the process $\pi N \rightarrow N e^+ e^-$ and presented numerical results for the anisotropy coefficient λ_θ based on the assumption that the process is dominated by intermediate baryon resonances. Our results show that the shape of the anisotropy coefficient λ_θ as a function of the scattering angle can provide information on the spin-parity of the intermediate baryon resonance.

We estimated the coupling constants in our model based on the information on decay widths of baryon resonances as given by the Particle Data Group. We find that at the HADES energy the cross section is dominated by the $N(1520)$ resonance and hence that the dilepton anisotropy reflects the $N(1520)$ with only a weak dependence on the model uncertainties.

The anisotropy coefficient can in principle be determined in experiments by the HADES collaboration at GSI, Darmstadt. To this end, at least a rough binning of the triple-differential dilepton production cross section is needed. This requires high statistics, which is not easily achieved for such a rare probe. On the other hand, the angular distributions provide valuable additional information, which can help disentangle the various contributions to the dilepton production cross section and thus also provide novel information on the properties of baryon resonances.

Several aspects of our model need to be improved in the future. First of all the model dependence of the predictions needs to be addressed. Repeating the calculation with a different choice for the ρ -baryon interaction Lagrangians, or a complementary approach, formulated in terms of helicity amplitudes or partial wave amplitudes, could provide a more systematic framework for exploring the various contributions to the scattering amplitude.

A previous study suggests that at the CM energy of the HADES experiment a significant part of the pion photoproduction cross section may be due to non-resonant Born contributions [3]. Consequently, these Born terms can influence also the angular distributions of dilepton production and the anisotropy coefficient in pion-nucleon collisions. Thus, their contribution to λ_θ should be assessed.

Additional constraints on the model could be provided by studying one-pion and two-pion production in pion-nucleon collisions, which have been measured at HADES with much better statistics than the dilepton final state.

Acknowledgments

The work of E.S. was supported by VH-NG-823, Helmholtz Alliance HA216/EMMI and GSI. M.Z. was supported by the Hungarian OTKA Fund No. K109462 and EMMI. The work of B.F. was partially supported by EMMI.

References

1. W. Przygoda (HADES Collaboration), JPS Conf. Proc. **10** (2016) 010013, Proceedings of the 10th International Workshop on the Physics of Excited Nucleons, NSTAR2015, May 25-28, 2015, Osaka, Japan; W. Przygoda (HADES Collaboration), talk presented at NSTAR2015.
2. E. Speranza, M. Zétényi and B. Friman, Phys. Lett. B **764** (2017) 282.

3. M. Zétényi and Gy. Wolf, Phys. Rev. C **86** (2012) 065209.
4. S. Y. Choi, T. Lee and H. S. Song, Phys. Rev. D **40** (1989) 2477.
5. N. M. Kroll, T. D. Lee and B. Zumino, Phys. Rev. **157** (1967) 1376.
6. T. Vrancx, L. De Cruz, J. Ryckebusch and P. Vancraeyveld, Phys. Rev. C **84** (2011) 045201.
7. K. A. Olive *et al.* [Particle Data Group Collaboration], Chin. Phys. C **38** (2014) 090001.
8. M. F. M. Lutz, G. Wolf and B. Friman, Nucl. Phys. A **706** (2002) 431 [Erratum-ibid. A **765** (2006) 431].